Dalton Transactions

Accepted Manuscript

This is an *Accepted Manuscript*, which has been through the Royal Society of Chemistry peer review process and has been accepted for publication.

Accepted Manuscripts are published online shortly after acceptance, before technical editing, formatting and proof reading. Using this free service, authors can make their results available to the community, in citable form, before we publish the edited article. We will replace this *Accepted Manuscript* with the edited and formatted *Advance Article* as soon as it is available.

You can find more information about *Accepted Manuscripts* in the Information for Authors.

ROYAL SOCIETY OF CHEMISTRY

www.rsc.org/dalton

Phosphine Substitution Reactions of (η^5- cyclopentadienyl)ruthenium bis(triarylphosphine) chloride, $CpRu(PAr_3)_2Cl$ {PAr_3 = PPh_3, $P(p\text{-}CH_3C_6H_4)_3$, $P(p\text{-}FC_6H_4)_3$, $P(p\text{-}CH_3OC_6H_4)_3$, and $PPh_2(p\text{-}CH_3C_6H_4)$}: A Tale of Two Mechanisms

Michael J. Verschoor-Kirss, [b] Olivia Hendricks [c], Lawrence Renna[a], David Hill [a], and Rein U. Kirss *,[a]

[a] Department of Chemistry and Chemical Biology, Northeastern University, Boston, MA 02115, [b] Department of Chemistry, Colby College, Waterville, ME 04901, [c] Department of Chemistry, Wellesley College, Wellesley, MA 02481. r.kirss@neu.edu

Abstract

The kinetics of phosphine substitution in $CpRu(PAr_3)_2Cl$ by $PMePh_2$ under pseudo-first order conditions in $CDCl_3$ have been measured for PAr_3 = PPh_3, **1a**, PPh_2(*p*-tol), **1b**, P(*p*-tol)$_3$, **1c**, P(*p*-$CH_3OC_6H_4$)$_3$, **1d**, and P(*p*-FC_6H_4)$_3$), **1e**. Activation parameters characteristic of a dissociative pathway ($\Delta H^{\dagger}$= 110-124±2 kJ/mol, $\Delta S^{\dagger}$ = 16-44±5-12 J/mol-K) are observed for all five compounds. The rate of substitution in $CpRu(PAr_3)_2Cl$ (**1a**) and $CpRu[P(p\text{-}FC_6H_4)_3]_2Cl$ (**1e**) is independent of added chloride ion and decreases in the presence of excess PAr_3, however, the rate of substitution in $CpRu[P(p\text{-}CH_3OC_6H_4)_3]_2Cl$ (**1d**) is first order in added chloride ion and is less dependent on added PAr_3. A mechanism involving $[CpRu(PAr_3)_2(PMePh_2)]^+[Cl]^-$ intermediates contributes to the substitution in **1b-d.**

Introduction

Cyclopentadienyl ruthenium (II) complexes of general formula $CpRu(PAr_3)_2Cl$ (where Ar = Ph, *p*-FC_6H_4, *p*-$CH_3OC_6H_4$, *m*-$CH_3C_6H_4$) are active as catalysts in a variety of carbon-carbon and carbon-nitrogen bond forming reactions, including the cyclization of propargylic alcohols, [1] the methylation of primary amines, [2] the dimerization of diazo compounds and the olefination of aldehydes and styrene. [3] The steric and electronic properties of the PAr_3 ligand affect the rate and the product distribution in these reactions. Phosphine dissociation and Ru-Cl bond solvolysis are both likely mechanistic steps in these reactions. Despite the utility of $CpRu(PAr_3)_2Cl$ compounds in catalysis, surprisingly little data is available about their rates of phosphine substitution. Kinetic data for phosphine substitution in $CpRu(PPh_3)_2Cl$, $Cp^*Ru(PMe_3)_2Cl$, (η^5-indenyl)$Ru(PPh_3)_2Cl$ and (η^5-pentadienyl)$Ru(PPh_3)_2Cl$ by $PMePh_2$ under pseudo-first order conditions is consistent with a dissociative mechanism. [4, 5, 6] In our studies of phosphine substitution in **1a-e** (equation 1) under pseudo-first order conditions in $CDCl_3$ we find that **1a** and **1e** behave differently from **1b-d**: the substitution rate in **1d** is largely independent of added PAr_3 and increases for both **1c** and **1d** in the presence of excess chloride ion. We suggest that a mechanism involving $[CpRu(PAr_3)_2)(PMePh_2)]^+[Cl]^-$ intermediates contributes to the substitution in **1c-d.** The observed rate acceleration in the presence of excess chloride ion may lead to new applications of $CpRu(PAr_3)_2Cl$ compounds as catalysts.

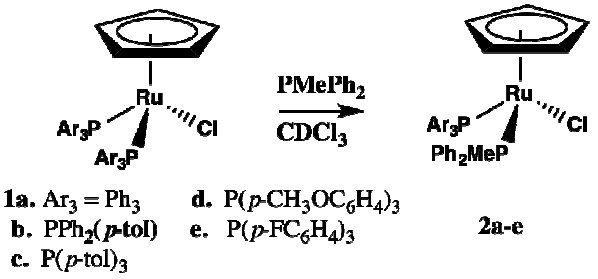

(1)

Experimental

All compounds described in this work were handled using Schlenk techniques or a M. I. Braun glove box under purified nitrogen atmospheres. [7] $RuCl_3$•x H_2O was purchased from Alfa Inorganics, Inc. Tertiary phosphines, $PMePh_2$, PPh_3, P(*p*-$CH_3C_6H_4)_3$, P(*p*-$CH_3OC_6H_4)_3$, P(*p*-$FC_6H_4)_3$, and PPh_2(*p*-$CH_3C_6H_4$) were obtained from Strem Chemical, Inc. and used as received. Anhydrous tetrabutylammonium halides, $^nBu_4Cl$ and $^nBu_4NI$, were purchased from Acros and dried under vacuum for 24 hours prior to use. Solvents were purified by refluxing over Na/benzophenone (toluene, tetrahydrofuran, benzene, hexane, pentane) or P_2O_5 (dichloromethane) and distilled prior to use. Benzene-d^6 (Cambridge Isotope Laboratories) and chloroform-d (Acros) were purified by refluxing over Na/benzophenone and P_2O_5, respectively, and distilled prior to use. Ruthenium (II) compounds $CpRu(PPh_3)_2Cl$ (**1a**), [8] $CpRu(PPh_2\{p\text{-}CH_3C_6H_4\})_2Cl$ (**1b**), [9] $CpRu(P\{p\text{-}CH_3C_6H_4\}_3)_2Cl$ (**1c**), [10] $CpRu(P\{p\text{-}CH_3OC_6H_4\}_3)_2Cl$ (**1d**), [11] $CpRu(P\{p\text{-}FC_6H_4\}_3)_2Cl$ (**1e**), [12] and $CpRu(PPh_3)(PMePh_2)Cl$ (**2a**), [13] were prepared by literature procedures. Melting points were determined in capillary tubes on an Electrothermal 9110 melting point apparatus and are uncorrected. Elemental analyses (C, H) were performed by Columbia Analytical Services, Inc. Tucson, AZ.

NMR spectra were recorded at 400 MHz for ^1H, and 162 MHz for $^{31}P\{^1H\}$ on a Varian XL300 spectrometer. Proton chemical shifts are reported relative to residual

protons in the solvent (CD_2**H**Cl at δ 7.24 ppm relative to TMS at 0.00 ppm). Phosphorus chemical shifts are reported relative to 85% H_3**P**O_4 at 0.0 ppm.

Electrochemical measurements were made under nitrogen on a BAS 100 B/W electrochemical workstation at 22°C using 1 x 10^{-3} M solutions in dry CH_2Cl_2, 0.1 M $^nBu_4NPF_6$ as supporting electrolyte at a scan rate of 100mV/s. The working electrode was a 3 mm Pt disk with a Pt wire as auxiliary electrode. A silver wire was used as a pseudo-reference electrode with ferrocene added as an internal standard with all potentials referenced to ferrocene ($E_{1/2}$ = 0.00 V).

Synthesis of CpRu(PAr$_3$)(PMePh$_2$)Cl (PAr$_3$ =P{p-CH$_3$C$_6$H$_4$}$_3$, P{p-FC$_6$H$_4$}$_3$, P{p-CH$_3$OC$_6$H$_4$}$_3$, and PPh$_2${p-CH$_3$C$_6$H$_4$})

General Procedure

Equimolar amounts of CpRu(PAr$_3$)$_2$Cl (**1a-e**) and PMePh$_2$ were refluxed in toluene or THF for 16 h. Solvent was removed in vacuo and the residue dissolved in a minimum of CH_2Cl_2. After filtering through a thin pad of neutral alumina, the product was precipitated with petroleum ether. Further purification was achieved by chromatography on neutral alumina with dichloromethane.

*CpRu(PPh$_2${p-CH$_3$C$_6$H$_4$},)(PMePh$_2$)Cl (***2b**)

Yellow-orange solid, 59% yield. M. p. 120-121°C.

Calculated for $C_{37}H_{35}P_2RuCl{\bullet}CH_2Cl_2$: 59.81%C, 4.89% H; Found: 60.06% C, 5.48% H

^{1}H (400 MHz, $CDCl_3$) δ 1.13 d (J = 8.8 Hz, 3H, PCH_3), 2.33 s (3H, CH_3), 4.16 s (5H, Cp), 5.30 s (2H, CH_2Cl_2), 7.03-7.7 m (28 H, aryl).

^{31}P (400 MHz, $CDCl_3$) δ 42.9 d (J_{PP}= 43 Hz), 29.9 d (J_{PP}= 43 Hz).

*CpRu(P{p-$CH_3C_6H_4$}$_3$)(PMePh_2)Cl (***2c**)

Yellow-orange solid, 60% yield. M. p. decomposes above 143°C.

Calculated for $C_{39}H_{39}P_2RuCl$: 66.53 %C, 5.57 % H; Found: 66.30 % C, 5.56 % H

^{1}H (400 MHz, $CDCl_3$) δ 1.13 d (J = 8.8 Hz, 3H, PCH_3), 2.32 s (9H, CH_3), 4.15 s (5H, Cp), 7.03-7.7 m (28 H, aryl)

^{31}P (400 MHz, $CDCl_3$) δ 41.3 d (J_{PP} = 43 Hz), 30.3 d (J_{PP} = 43 Hz).

*CpRu(P{p-$CH_3OC_6H_4$}$_3$)(PMePh_2)Cl (***2d**)

Yellow-orange solid, 90% yield. M. p. turns dark brown without melting 159-161°C.

When the product is crystallized from CH_2Cl_2/hexane, it retains one equivalent of CH_2Cl_2 by elemental analysis and ^{1}H NMR: Calculated for $C_{39}H_{39}O_3P_2RuCl$: 62.11 %C, 5.20 % H; Found: 61.66 % C, 5.47 % H.

^{1}H (400 MHz, $CDCl_3$) δ 1.16 d (J = 8.8 Hz, 3H, PCH_3), 3.80 s (9H, CH_3O), 4.16 s (5H, Cp), 7.13 -7.7 m (28 H, aryl).

^{31}P (400 MHz, $CDCl_3$) δ 39.5 d (J_{PP} = 43 Hz), 30.7 d (J_{PP} = 43 Hz).

*CpRu(P{p-FC_6H_4}$_3$)(PMePh_2)Cl (***2e**)

Orange solid, 62% yield. M. p. turns dark brown without melting 151-153°C.

Calculated for $C_{36}H_{30}F_3P_2RuCl$: 60.21 %C, 4.21 % H; Found: 60.22% C, 4.99 % H

^{1}H (400 MHz, $CDCl_3$) δ 1.19 d (J = 8.8 Hz, 3H, PCH_3), 4.19 s (5H, Cp), 6.9-7.7 m (28 H, aryl).

^{31}P (400 MHz, $CDCl_3$) δ 43.4 d (J_{PP} = 44 Hz), 30.4 d (J_{PP} = 44 Hz).

*Kinetic measurements for reaction of **1a-e** with PMe_2Ph*

Stock solutions of the ruthenium complexes were prepared by dissolving an appropriate amount of **1a-e** in 10.0 mL $CDCl_3$ in volumetric flasks in an inert atmosphere glove box. Addition of 300-350 μL $PMePh_2$ yields solutions with ruthenium concentrations between 12 and 18 mM and $PMePh_2$ concentrations between 150 and 190 mM. Samples for the kinetic experiments were prepared by transferring 600 μL of the stock solution to 5 mm NMR tubes attached to 14/20 ground glass joints. The tubes were flame-sealed sealed under vacuum. Samples were stored at -20°C. No reaction is observed at this temperature over a minimum of two months. For the kinetics experiments, NMR tubes containing solutions of **1a-d** were heated in thermostated water baths at 25.3± 0.2, 30.4±0.2, 35.1±0.2 and 40.3±0.2°C. The tubes were removed from the bath, cooled to 0°C and evaluated by ^{31}P NMR in a probe maintained at 20±1°C. The same procedures applied to samples of **1e** with the exception that thermostated oil baths at 25±1, 40±1, 45±1 and 50±1°C were used in place of water baths. The choice of a relatively narrow temperature change for the kinetic measurements is predicated by the acquisition times required for each spectrum (between 15 and 20 minutes depending on the concentration of the sample), the ability to accurately control reaction temperatures below 25°C and the rates of reaction at temperatures above 40°C. These times were taken into account when calculating the activation parameters.

The rate of substitution of PPh_3 by PMe_2Ph was measured by monitoring the decrease in the singlet for (η^5-C_5H_5)Ru (PAr_3)$_2$Cl (**1a-e**) in the ^{31}P NMR spectra over

time relative to the doublets for (η^5-C_5H_5)Ru(PAr_3)($PMePh_2$)Cl (**2a-e**). Three independent measurements of the substitution rate were made at each temperature to determine the observed rate constant (k_{obs}) for the reaction. Additional series of experiments were performed using **1d-e** and PMe_2Ph concentrations between 310 mM and 210 mM.

Activation parameters were determined using the Eyring equation by plotting ln (k_{obs}/T) vs 1/T where the slope = $-\Delta H^{\dagger}/R$ and the intercept = $\Delta S^{\dagger}/R + \ln k_B/h$. It has been argued that values for activation entropy, $\Delta S^{\dagger}$, calculated from the Eyring equation are inaccurate because extrapolation to T=0 K is required. To address this issue, it is also possible to evaluate $\Delta S^{\dagger}$ from the slope of a plot of T ln(k/T) vs T. For comparison, $\Delta S^{\dagger}$ and $\Delta H^{\dagger}$ were obtained from the slope and intercept from a plot of T ln (k_{obs}/T) vs 1/T. [14] The same values for $\Delta S^{\dagger}$ were obtained using each method. Errors in $\Delta S^{\dagger}$ and $\Delta H^{\dagger}$ were calculated using the statistical packages in Excel and by procedures described in standard analytical chemistry texts.[15]

To investigate the effect of PAr_3 on the substitution rate flame-sealed NMR tubes were prepared by adding stock solutions containing **1a-e** (15 mM) and $PMePh_2$ (150mM) to volumetric flasks containing 2.5-225 mM (0.2-15 eq) PAr_3 as described above. A similar set of tubes were prepared by adding stock solutions of **1a-e** (15 mM), $PMePh_2$ (150mM) to volumetric flasks containing 2.5-165 mM (0.2-11 eq) $^nBu_4X$ (X = Cl, I).

Computational Methods

All calculations were conducted using density functional theory (DFT) as implemented in the Gaussian09 Revision B.01 suite of ab initio quantum chemistry programs [16]. Normal

self-consistent field (SCF) and geometry convergence criteria were employed and structures were optimized in the gas phase without the use of symmetry constraints. Harmonic frequency analysis based on analytical second derivative was used to characterize optimized structures as local minima on the potential energy surface.

Geometry optimizations and vibrational frequency calculations were performed by using the unrestricted B3LYP exchange and correlation functional [17-19] and the double-ζ DGDZVP basis set [20-21] for all atoms. Relative energies including solvation were evaluated [22-23] by performing self-consistent reaction field (SCRF) calculations on the optimized gas phase geometry using the integral equation formalism polarizable continuum model (IEFPCM) initially developed by Tomasi and co-workers. [24] In this dielectric continuum model, the solute is placed in a cavity within the solvent continuum with solute-solvent boundary defined by using a solvent excluding surface (SES). [25] The molecular solute surface was defined by using the United Atom Topological model (UAHF) for the radii of the solute atoms. [26] A chloroform solvent continuum model using standard parameters ($\varepsilon = 4.7113$, $R_{solv} = 2.4800$ Å) where ε is the dielectric constant and R_{solv} is the sphere radius of the solvent. Gaussian03 default settings [16] were used to calculate relative free energy including solvation, ΔG / kJ mol^{-1}. The choice of solvation model reflects the method used for kinetic measurements ($CDCl_3$). Optimized structures were analyzed by using Chemcraft (version 1.7, build 365).

Results

The rate of reaction between **1a-e** and ≈ 10 equivalents of $PMePh_2$ in $CDCl_3$ is readily monitored by ^{31}P NMR and follows first order kinetics over four to five half-lives, yielding a single product in all cases: $CpRu(PAr_3)(PMePh_2)Cl$ (**2a-e**). The singlet

resonance for the starting materials is slowly replaced by two well resolved doublets of $CpRu(PAr_3)(PMePh_2)Cl$ with the appearance of free PAr_3. With the exception of small amounts of $O{=}PMePh_2$, no additional signals are seen in the final spectra. During the reaction, however, spectra of **1c** and **1d** contain a doublet and a triplet of very weak intensity that disappear by the end of the reaction. For **1c**, these signals appear at δ 35.8 d (J_{PP} = 38 Hz) and δ 7.91 t (J_{PP} = 38 Hz) while for **1d** these resonances appear at δ 34.3 d (J_{PP} = 39 Hz) and δ 7.44 t (J_{PP} = 39 Hz). These resonances account for ≤ 3 % of the total area for all of the resonances in each sample. The relative intensity of these resonances for **1d** does not increase even upon addition of 100 equivalents $PMePh_2$. These resonances are not observed when THF is used as a solvent for **1a-e**.

The pseudo-first order rate constants (k_{obs} at 25°C) and activation parameters for equation 1 are listed in Table 1. An observed lack of reactivity for **1a-e** at 0°C and the slow rate of reactions at 25°C suggest a minimal effect of spectrometer residence time on the abscissa for the plots of ln[**1**] vs time used to calculate k_{obs}. Values for the activation entropy are positive and range from 16±7 to 66±5 J/mol-K. Reactions of the products **2a-e** with excess PAr_3 do not yield **1a-e**. The rate of substitution for **1a-e** decreases as [PAr_3] increases (Figure 1). For **1d**, however, the effect of [PAr_3] on the rate of substitution appears to be substantially less than for **1a-c** and **1e**. The substitution rates in **1a** and **1e** are independent of $PMePh_2$ concentration, however, for **1d**, an increase in rate is observed as [$PMePh_2$] increases (Figure 2).

Table 1: Pseudo first order rate constants and activation parameters for the substitution of PAr_3 by $PMePh_2$ in **1** in $CDCl_3$[a]

PAr_3	$k_{obs,\ 25°C}$ (x 10^6 s^{-1})	$\Delta H^{\dagger}$(kJ/mol)	$\Delta S^{\dagger}$(J/mol-K)
PPh_3 **1a**	5.49±0.06	123±2	66±5
PPh_2(*p*-tol), **1b**	4.93±0.04	121±2	59±6
P(*p*-tol)$_3$, **1c**	4.00±0.02	117±2	44±7
P(*p*-MeOC$_6$H$_4$)$_3$, **1d**	2.67±0.04	110±2	16±7
P(*p*-FC$_6$H$_4$)$_3$, **1e**	2.26±0.05	124±2	64±12

[a]Concentrations of reactants and products were determined from integration of the resonances. Concentrations of **1a-e** ranged from 12 to 18 mM with a ≈ 10 fold excess of $PMePh_2$.

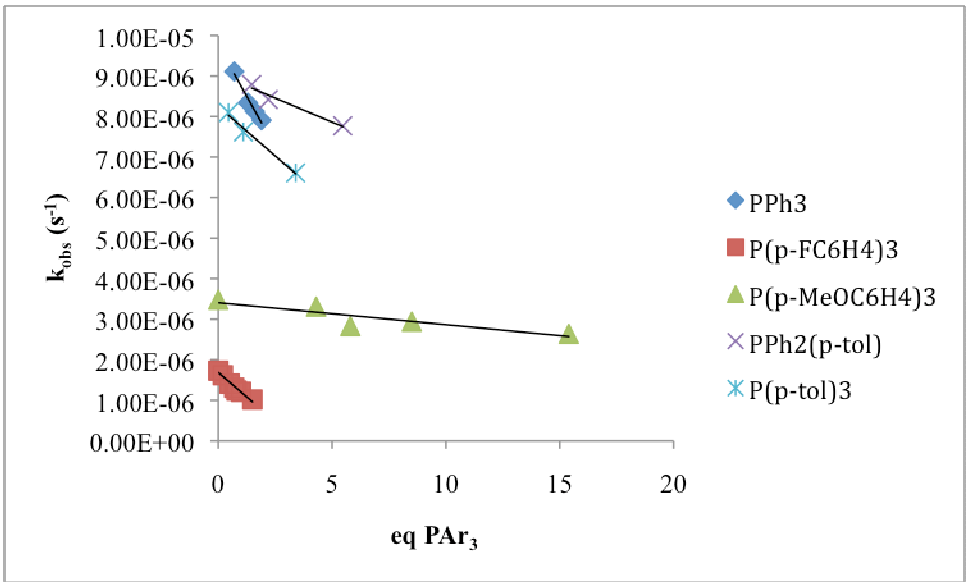

Figure 1: Dependence of k_{obs} on [PAr_3] for **1a-e**.

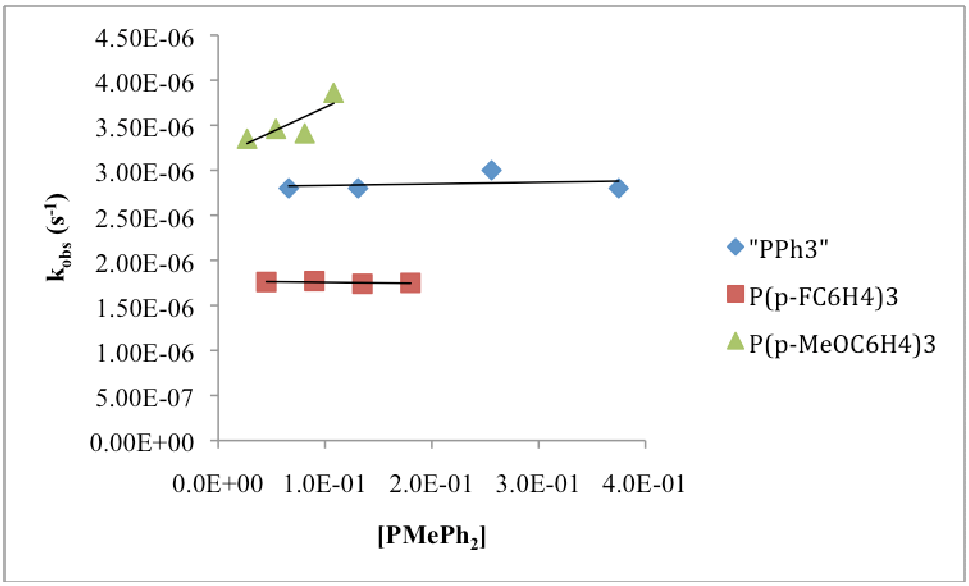

Figure 2: Dependence of k_{obs} on [$PMePh_2$] for **1a**[4], **1d** and **1e**.

The halide ligand in **1-e** is quite labile even in $CDCl_3$ solution. Reaction between **1a-e**, 10 equivalents of $PMePh_2$, and 10 equivalents of $^nBu_4NI$ results in varying degrees of halide exchange prior to phosphine substitution. In the case of **1c-d**, halide exchange is complete before any phosphine substitution is observed yielding $CpRu(PAr_3)(PMePh_2)I$ as the final product in the reaction. For **1a-b** and **1e**, $CpRu(PAr_3)_2I$, $CpRu(PAr_3)(PMePh_2)Cl$ and $CpRu(PAr_3)(PMePh_2)I$ are all observed in the reaction mixture with the ratio of $CpRu(PAr_3)(PMePh_2)I$ to $CpRu(PAr_3)(PMePh_2)Cl$ increasing from 2:1 for **1e** to 5:1 for **1a-b** at the end of the reaction.

The rate of phosphine substitution in **1a** and **1e** is unaffected by up to 10 equivalents of added Cl^-. Surprisingly, the rate of disappearance of **1b-d** *increases* with increasing chloride concentration (Figure 3). The degree of rate enhancement tracks with increasing basicity (σ-donation) of PAr_3, with **1b** showing the smallest increase in rate and **1d** having the greatest increase in the phosphine substitution rate. A plot of ln k_{obs} vs

[Cl⁻] for **1d** is linear with a slope of 0.998 consistent with a first order dependence of the rate on chloride ion. Under these conditions, significant amounts of $CpRu(PMePh_2)_2Cl$ (^{31}P δ 31.1 s) are observed in the ^{31}P NMR spectra of the reaction mixtures containing **1b-d**, $^{n}Bu_4NCl$, and $PMePh_2$. Furthermore, the intensity of the minor resonances seen in the spectra of **1c** and **1d,** (δ 35.8 d, 7.91 t and δ 34.3 d, 7.44 t, respectively) increase in intensity as halide concentration increases. No changes are seen in the ^{31}P NMR spectrum of **1d** when 100 eq. of $^{n}Bu_4NCl$ (but no $PMePh_2$) is added.

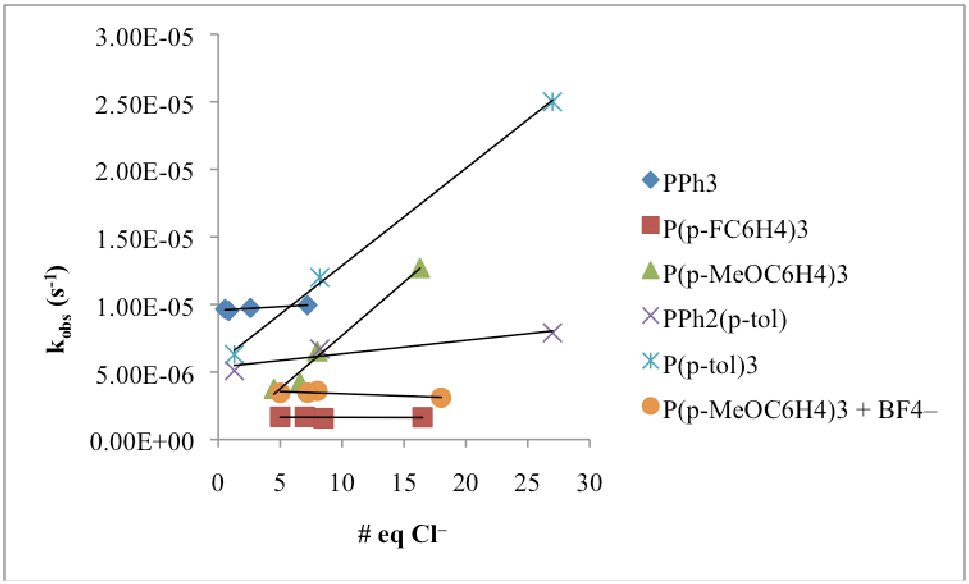

Figure 3: Plots of k_{obs} vs [Cl⁻] for **1a-e** and a plot of k_{obs} vs [BF_4^-] for **1d**.

DFT calculations were used to evaluate the relative free energies of potential intermediates in the substitution reaction (Figure 4, for PAr_3 = PPh_3 and Table 2 for **1a** and **1d-e**). The data in Figure 4 indicate the relative free energies of potential intermediates in the reaction and do not represent activation energies. Sixteen electron intermediates, $CpRu(PAr_3)Cl$, have similar calculated Gibbs free energies, ≈ 40-50

kJ/mol above that for the relative free energy of solvated $CpRu(PAr_3)_2Cl$, **1a** and **1d-e.** Cationic intermediates, $[CpRu(PAr_3)_2(PMePh_2)]^+$, all have calculated free energies lower than the starting material with $[CpRu\{P(p\text{-}MeOC_6H_4)_3\}_2(PMePh_2)]^+$ the most stable, some ≈ 60-70 kJ/mol lower in energy than $[CpRu(PPh_3)_2(PMePh_2)]^+$ or $[CpRu\{P(p\text{-}FC_6H_4)_3\}_2(PMePh_2)]^+$. The data in Table 2 also reveal that $[CpRu\{P(p\text{-}MeOC_6H_4)_3\}_2]^+$, formed by halide dissociation from **1d**, is between 8 and 33 kJ/mol thermodynamically more stable than the corresponding $[CpRu(PAr_3)_2]^+$, derived from **1a** or **1e**.

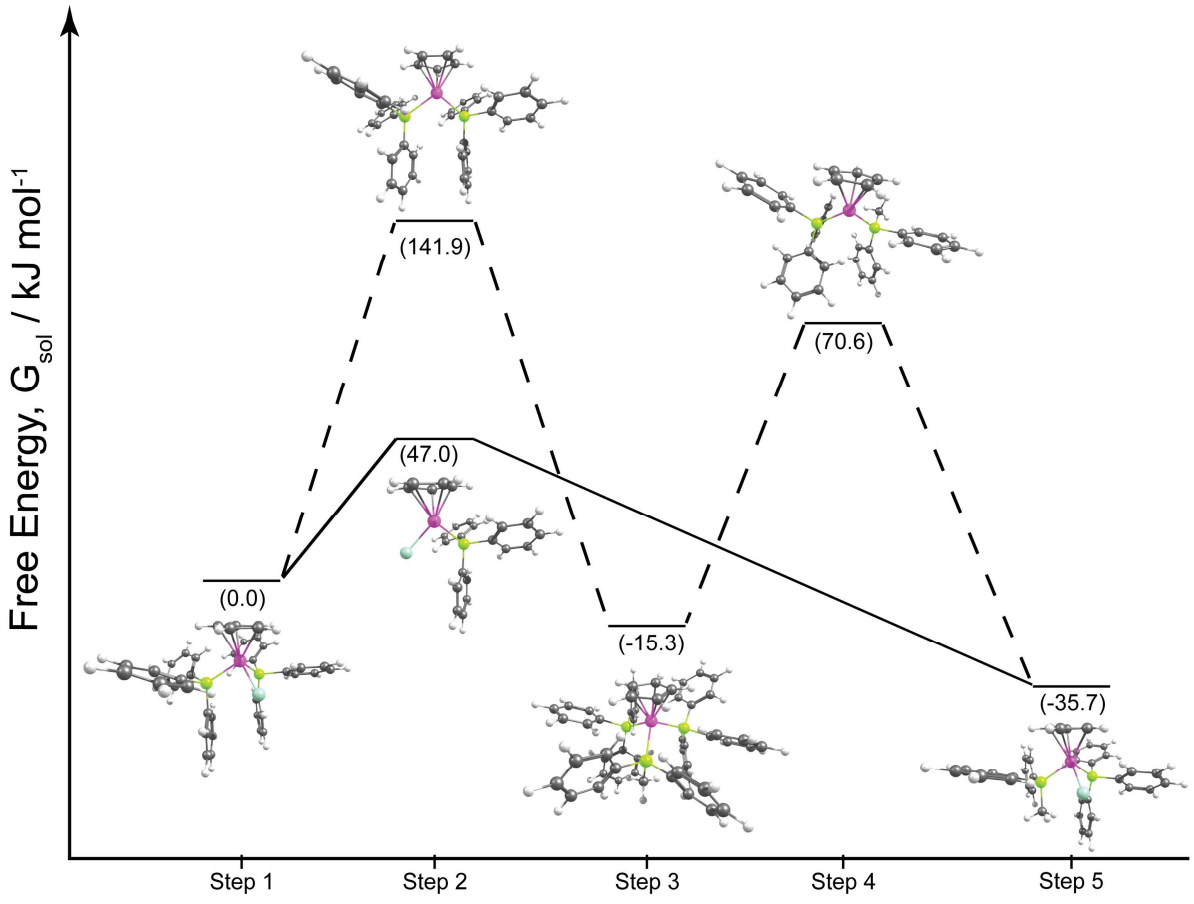

Figure 4: DFT calculated reaction coordinate showing changes in the Gibbs free energy including solvation for step-wise conversion of $CpRu(PPh_3)_2Cl$ to $CpRu(PPh_3)(PPh_2Me)Cl$ along pathways A (solid line) and B (dashed line). Relative

energies including solvation were determined from single point gas phase optimized geometries.

Table 2: Calculated Gibbs Free Energies (kJ/mol) for Possible Intermediates in the Phosphine Substitution Reactions of **1a**, and **1d-e**†

Pathway A: Phosphine Dissociation	$P(C_6H_5)_3$ **1a**	$P(p\text{-}CH_3OC_6H_4)_3$ **1d**	$P(p\text{-}FC_6H_4)_3$ **1e**
$RuCp(PAr_3)_2Cl + PPh_2Me \Leftrightarrow RuCp(PAr_3)Cl + PAr_3 + PPh_2Me$	47.1	41.3	50.5
$RuCp(PAr_3)Cl + PAr_3 + PPh_2Me \Leftrightarrow RuCp(PAr_3)(PPh_2Me)Cl + PAr_3$	-35.7	-31.3	-33.7
Pathway B: Halide Dissociation	$P(C_6H_5)_3$ **1a**	$P(p\text{-}CH_3OC_6H_4)_3$ **1d**	$P(p\text{-}FC_6H_4)_3$ **1e**
$RuCp(PAr_3)_2Cl + PPh_2Me \Leftrightarrow [RuCp(PAr_3)_2]^+ + Cl^- + PPh_2Me$	141.9	133.4	166.1
$[RuCp(PAr_3)_2]^+ + Cl^- + PPh_2Me \Leftrightarrow [RuCp(PAr_3)_2(PPh_2Me)]^+ + Cl^-$	-15.2	-72.7	-2.2
$[RuCp(PAr_3)_2(PPh_2Me)]^+ + Cl^- \Leftrightarrow [RuCp(PAr_3)(PPh_2Me)]^+ + Cl^- + PAr_3$	99.2	96.6	113.9
$[RuCp(PAr_3)(PPh_2Me)_1]^+ + Cl^- + PAr_3 \Leftrightarrow RuCp(PAr_3)(PPh_2Me)Cl + PAr_3$	-35.7	-31.3	-33.7

† Relative energies including solvation were determined from single point gas phase optimized geometries.

Discussion

The data for the reaction rate of **1a-e** with $PMePh_2$ in $CDCl_3$ (Table 1) span a relatively small range of values. The cone angles for the PAr_3 ligands, [27] are all similar,

eliminating any steric effect of PAr_3 ligands on the substitution rate. With the exception of **1e** (PAr_3 = $P(p\text{-}FC_6H_4)_3$), the rate constants decrease with increasing σ-donation (basicity) of the PAr_3 ligand as reflected by both the pK_a of PAr_3 [28] and the electrochemical potentials for **1a-e** (Table 3). A Hammett plot of k_{obs} vs σ_p for **1a, c** and **d** is linear (no value for σ_p for **1b** is available). [29] The value of k_{obs} for **1e**, however, does not fit the trend on this plot; one would predict a much faster rate than observed. The slow rate for **1e** and similarity of k_{obs} for **1d** and **1e** is surprising and suggests a mechanistic difference in the reaction of **1e** with $PMePh_2$.

Two mechanisms for phosphine substitution are suggested by the literature: dissociation of PAr_3 (path A in Figure 5) followed by addition of $PMePh_2$ and displacement of Cl^- by $PMePh_2$ (path B) followed by loss of PAr_3. Each of these mechanisms will show a different response to changing the [$PMePh_2$], [PAr_3] and [Cl^-].

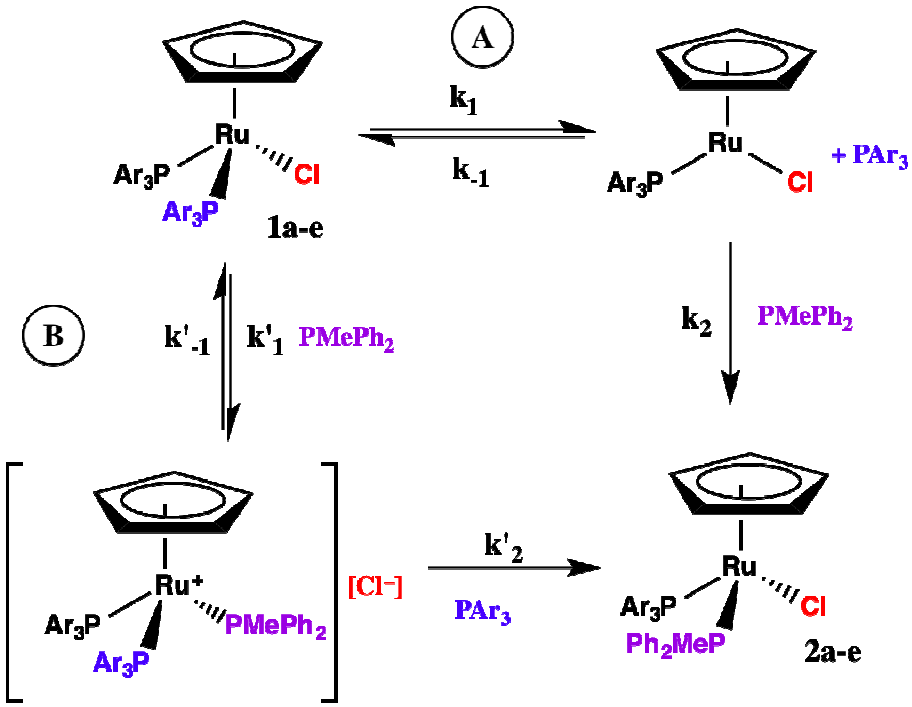

Figure 5: Possible Mechanisms for Phosphine Substitution in **1a-e**

The data for **1d** and **1e** are consistent with pathway B and A, respectively. Substitution in **1e** is independent of the [$PMePh_2$] and [Cl^-] while decreasing as [PAr_3] increases. These observations are consistent with a dissociative mechanism in Figure 5 (Path A) and the rate law in equation 2; a rate decrease in the presence of added PAr_3, is expected for a dissociative or dissociative interchange pathway in Figure 5 where dissociation of PAr_3 is the rate-determining step. [30] The positive activation entropy ($\Delta S^{\dagger} > 0$) supports a dissociative or dissociative interchange pathway and is similar to that reported for **1a** in THF (equation 1). [4] Since halide loss does not occur in path A, changing the concentration of chloride should have no effect on the rate, consistent with the data in Figure 3. Furthermore, no resonances other than **1e**, **2e**, $PMePh_2$ and PAr_3 are seen in the spectra at any time during the substitution reaction.

$$Rate = k_{obs}[CpRu(PAr_3)_2Cl] \qquad k_{obs} = \frac{k_1 k_2 [PMePh_2]}{k_{-1}[PAr_3] + k_2[PMePh_2]} \quad (2)$$

Table 3: Electrochemical Potentials, Cone Angles and pK_a for $CpRu(PAr_3)_2Cl$ **1a-e**.[†]

PAr_3	E° (mV)	Φ (°)[27]	pK_a[28]
$P(p\text{-}FC_6H_4)_3$	186	145	1.97
PPh_3	140	145	2.73
$PPh_2(p\text{-tol})$	41	145	
$P(p\text{-tol})_3$	23	145	3.84
$P(p\text{-}MeOC_6H_4)_3$	-18	145	4.57

[†]1 x 10^{-3} M solutions in dry CH_2Cl_2 with 0.1 M $^nBu_4NPF_6$ as supporting electrolyte at 22°C and a scan rate of 100mV/s.

The reaction of **1d** is also first order in the presence of excess $PMePh_2$ (pseudo-first order conditions). The rate of reaction for **1d** decreases as [PAr_3] increases, however, the rate of substitution seems much less dependent on [P(*p*-$CH_3OC_6H_4)_3$] than for **1e** (Figure 1). An increase in the reaction rate with increasing [$PMePh_2$] (Figure 2) is more consistent with an equilibrium between **1d** and [CpRu{P(*p*-$MeOC_6H_4)_3$}$_2$($PMePh_2$)]$^+$[Cl]$^-$ followed by phosphine dissociation as the rate determining step and the rate law in equation 3 (Path B in Figure 5).

$$Rate = k_{obs}[CpRu(PAr_3)_2Cl] \qquad k_{obs} = \frac{k'_1 k'_2[PMePh_2]}{k'_{-1} + k'_2} \qquad (3)$$

If the second step in path B is rate determining, then small concentrations of the intermediate, [CpRu{P(*p*-$MeOC_6H_4)_3$}$_2$($PMePh_2$)]$^+$[Cl]$^-$, should be detected in the reaction of **1d** with $PMePh_2$ in $CDCl_3$. Indeed, doublet (δ 34.3 ppm, J_{PP} = 39 Hz, 2 P) and triplet (δ 7.44 ppm, J_{PP} = 39 Hz, 1 P) resonances seen throughout the experiment are consistent with the presence of small amounts of a ruthenium compound bearing two PAr_3 ligands and one $PMePh_2$ ligand. We assign these resonances to a CpRu(PAr_3)$_2$($PMePh_2$)$^+$ cation rather than a neutral η^3-CpRu(PAr_3)$_2$($PMePh_2$)Cl species, given that the halide in **1d** is quite labile. The results of DFT calculations confirm that [CpRu{P(*p*-$MeOC_6H_4)_3$}$_2$($PMePh_2$)]$^+$ is quite stable, with a calculated free energy of –73 kJ/mol relative to **1d**. Although the rate of reaction depends on [$PMePh_2$], the intensity of the resonances for CpRu(PAr_3)$_2$($PMePh_2$)$^+$ do not increase significantly with increasing [$PMePh_2$] even when 100 equivalents of $PMePh_2$ are present suggesting that the equilibrium constant in $CDCl_3$, k_1'/k'_{-1}, is small. With the exception of

$Cp^*Ru(PMe_3)_3^+$, [31] we are not aware of any cyclopentadienyl ruthenium cations with three phosphine ligands. Related compounds, $[\eta^5\text{-indenylRu}(PPh_3)(dppm)]^+[Cl]^-$ and $[\eta^5\text{-indenylRu}(PPh_3)(dppe)]^+[Cl]^-$, precipitate out of toluene solution and lose PPh_3 when refluxed for two hours. [4]

The response of k_{obs} to increasing chloride concentration in reactions of **1d** is very different from that observed for **1e**. The substitution of $PMePh_2$ for PAr_3 in **1d** is first order in $[Cl^-]$. The concentration of the cationic intermediate, $[CpRu\{P(p\text{-}MeOC_6H_4)_3\}_2(PMePh_2)]^+$, increases as the concentration of chloride increases consistent with an increase in the equilibrium constant k_1'/k_{-1}' as the dielectric constant of the solution changes. While $CDCl_3$ is not a particularly strong Lewis base, it is a polar solvent capable of dissolving cationic compounds to some degree. These observations also suggest that the intermediate is indeed a cationic, $[CpRu\{P(p\text{-}MeOC_6H_4)_3\}_2(PMePh_2)]^+$ species and not neutral $\eta^3\text{-}CpRu[P(p\text{-}MeOC_6H_4)_3]_2(PMePh_2)Cl$. The apparent effect of chloride ion is to accelerate the displacement of PAr_3 from the $[CpRu(PAr_3)_2(PMePh_2)]^+$ cation in a bimolecular rate determining step. An explanation of the data based on a kinetic salt effect is unlikely since added $[NMe_4][BF_4]$ has *no effect* on the substitution rate in **1d** (Figure 3).

The mechanism in Figure 5 does not, by itself, entirely explain the observed increase in substitution rate in **1d** as a function of increased chloride ion concentration. There is no chloride term in the rate law in equation 3 and the rate determining step for pathway B in the absence of added halide may simply involve dissociation from a cationic species $[CpRu\{P(p\text{-}MeOC_6H_4)_3\}_2(PMePh_2)]^+$. The role of the nucleophile (Cl^-) in the substitution reactions of **1d** suggests a different mechanism from those in Figure 5.

Although the role of Cl^- in the loss of PAr_3 from $CpRu(PAr_3)_2(PMePh_2)^+$ (or even $CpRu(PAr_3)_2Cl$) is not clear, it has been suggested that phosphine ligands bear part of the positive charge in cationic transition metal phosphine compounds that can lead to weak ion-pairing effects with anions such as chloride. [32] High concentrations of halide ion may result in nucleophilic attack by halide ion on a coordinated phosphine ligand since only a good nucleophile like Cl^- accelerates the rate of phosphine substitution in **1d**; a non-coordinating anion, BF_4^-, has no effect the reaction rate despite changing the ionic strength of the solution.

Conclusions

The kinetic study of phosphine substitution in $CpRu(PAr_3)_2Cl$ (**1a-e**) with $PMePh_2$ in $CDCl_3$ reveals two competing mechanisms for the reaction that depend on the electronic properties of PAr_3. For **1e** (Ar = p-FC_6H_4), phosphine dissociation is preferred. As the σ-basicity of PAr_3 increases, formation of ionic intermediates, $[CpRu(PAr_3)_2(PMePh_2)]^+$ becomes increasingly important. Evidence for cationic $[CpRu(PAr_3)_2(PMePh_2)]^+$ intermediates is strongest for **1d** (Ar = *p*-$MeOC_6H_4$) where resonances consistent with a cationic species persist through much of the reaction and where the reaction is first order in chloride. The results of DFT calculations support that viability of $[CpRu\{P(p\text{-}CH_3OC_6H_4)_3\}_2(PMePh_2)]^+$ as an intermediate in the reaction of **1d** with $PMePh_2$ whereas there seems to be no thermodynamic advantage gained in the formation of $[CpRu\{P(p\text{-}FC_6H_4)_3\}_2(PMePh_2)]^+$. Thus, the near equivalence of the rate constants for $CpRu\{P(p\text{-}CH_3OC_6H_4)_3\}_2Cl$ (**1d**) and $CpRu\{P(p\text{-}FC_6H_4)_3\}_2Cl$ (**1e**) is most likely coincidental.

The kinetic data for compounds **1b-c** suggest that both mechanisms likely operate in both of these compounds. The substitution reactions are all first order in ruthenium and inhibited by added PAr_3 to a different degree, with **1c** less affected by increasing [PAr_3] than **1a-b** but showing a greater response than **1d**. The rate of reaction increases as [Cl^-] increases for **1b** and **1c** but fractional reaction orders are observed. Clearly, modeling of the rates will be helpful in further probing the mechanism, however, the data do seem consistent with the interpretation of competing mechanisms.

Supplementary Information

Acknowledgments The authors wish to thank Dr. Jason P. Holland (Massachusetts General Hospital) for his assistance with the computational chemistry (DFT).

Author Information

Corresponding author: r.kirss@neu.edu

References

1. a. Trost, B. M.; Rhee, Y. H. *J. Amer. Chem. Soc.* **2002**, 12,4 2528-2533; b. Trost, B. M.; Malhotra, S.; Mino, T.; Rajapaksa, N. S. *Chem. Eur. J.* **2008**, *14*, 7648-7657.
2. Del Zotto, A.; Barrata, W.; Sandri, M.; Verardo, G.; Rigo, P. *Eur. J. Inorg. Chem.* **2004**, 524-529.
3. a. Barrata, W.; Del Zotto, A.; Rigo, P. *Organometallics* **1999**, *18*, 5091-5096; b. Barrata, W.; Herrmann, W. A.; Kratzer, R. M.; Rigo, P. *Organometallics*, **2000**,

19, 3664-3669; c. Kuhn, F. E.; Santos, A. M.; Jogalekar, A. A.; Pedro, F. M.; Rigo, P.; Baratta, W. *J. Catal*. **2004**, *227*, 253-256; d. Pedro, F. M.; Santos, A.M.; Baratta, W.; Kuhn, F. E. *Organometallics* **2007**, *26*, 302-309.

4. Gamasa, M. P.; Gimeno, J.; Gonzalez-Bernardo, C.; Martin-Vaca, B. M.; Monti, D.; Bassetti, M. *Organometallics* **1996**, *15,* 302-308.
5. Daniels, M.; Kirss, R. U. *J. Organometallic Chem.* **2007**, *692*, 1716-1725.
6. Bryndza, H. E.; Domaille, P. J.; Paciello, R. A.; Bercaw, J. E. *Organometallics* **1989**, *8*, 379-385.
7. Shriver, D.F. *Manipulation of Air Sensitive Compounds* McGraw Hill; New York **1969**.
8. a. Bruce, M. I.; Hameister, C.; Swincer, A. G.; Wallis, R. C. *Inorg. Synth.* **1990**, *28*, 270-272; b. Bruce, M. I.; Hameister, C.; Swincer, A. G.; Wallis, R. C.; Ittel, S. D. *Inorg. Synth.* **1982**, *21*, 78-84.
9. Costello, J. F.; Davies, S. G.; Highcock, R. M. Polywka, M. E.; Poulter, M. W.; Richardson, T.; Roberts, G. G. *J. Chem. Soc. Dalton Trans.* **1997** 105-109.
10. Bruce, M. I.; Windsor, N. J. *Aust. J. Chem.* **1977**, *30*, 1601-1604.
11. Nataro, C.; Chen, J.; Angelici, R. J. *Inorg. Chem.* **1998**, *37*, 1868-1875.
12. Hartwig, J. F.; Bhandari, S.; Rablen, P. R. *J. Am. Chem. Soc.* **1994**, *116*, 1839-1844.
13. Treichel, P.M.; Komar, D. A. *Synth. React. Inorg. Met.-Org. Chem.* **1980**, *10*, 205-218.
14. Lente, G.; Fabian, I.; Poe, A.J. *New J. Chem.* **2005**, *29*, 759-760.

15. Skoog, D.A.; West, D.M.; Holler, J. *Analytical Chemistry: An Introduction,7th ed.* Saunders; NY **2000**.

16. Frisch, M. J.; Trucks, G. W.; Schlegel, H. B. ; Scuseria, G. E. ; Robb, M. A. ; Cheeseman, J. R.; Scalmani, G.; Barone, V.; Mennucci, B.; Petersson, G. A.; Nakatsuji, H.; Caricato, M.; Li, X.; Hratchian, H. P. ; Izmaylov, A. F.; Bloino, J.; Zheng, G.; Sonnenberg, J. L.; Hada, M.; Ehara, M.; Toyota, K.; Fukuda, R.; Hasegawa, J.; Ishida, M.; Nakajima, T.; Honda, Y.; Kitao, O.; Nakai, H.; Vreven, T.; Montgomery, J. J. A. ; Peralta, J. E.; Ogliaro, F.; Bearpark, M.; Heyd, J. J.; Brothers, E.; Kudin, K. N.; Staroverov, V. N.; Keith, T.; Kobayashi, R.; Normand, J.; Raghavachari, K.; Rendell, A.; Burant, J. C.; Iyengar, S. S.; Tomasi, J.; Cossi, M.; Rega, N.; Millam, J. M.; Klene, M.; Knox, J. E.; Cross, J. B.; Bakken, V.; Adamo, C.; Jaramillo, J.; Gomperts, R.; Stratmann, R. E.; Yazyev, O.; Austin, A. J.; Cammi, R.; Pomelli, C.; Ochterski, J. W.; Martin, R. L.; Morokuma, K.; Zakrzewski, V. G.; Voth, G. A.; Salvador, P.; Dannenberg, J. J.; Dapprich, S.; Daniels, A. D.; Farkas, O.; Foresman, J. B.; Ortiz, J. V.; Cioslowski, J.; Fox, D. J. *Gaussian 09 Revision B.01., Gaussian, Inc., Wallingford, CT.*, **2010**.

17. Lee, C.; Yang, W.; Parr, R. G. *Phys Rev. B,* **1988**, *37*, 785-789.

18. Becke, A. D. *Phys. Rev. A* **1988**, *38*, 3098-3100.

19. Stephens, P.J.; Devlin, F. J.; Chabalowski, C. F.; Frisch, M. J. *J. Phys. Chem.,* **1994**, *98*, 11623-11627.

20. Godbout, N.; Salahub, D. R.; Andzelm, J.; Wimmer, E. Can. J. Chem., **1992**, *70*, 560-571.

21. Sosa, C.; Andzelm, J.; Elkin, B. C.; Wimmer, E.; Dobbs, K. D.; Dixon, D. A. *J. Phys. Chem.,* **1992**, *96*, 6630-6636.

22. Hall, R. J.; Davidson, M. M. ; Burton, N. A.; Hillier, I. H. *J. Phys. Chem.,* **1995**, *99*, 921-924.

23. Chen, J. L.; Noodleman, L.; Case, D. A.; Bashford, D. *J. Phys. Chem.,* **1994**, *98*, 11059-11068.

24. Tomasi, J.; Mennucci, B.; Cammi, R. *Chem. Rev.* **2005**, *105*, 2999-3094.

25. Connolly, M. L. *Science,* **1983**, *221*, 709-713.

26. Adamo, C.; Barone, V. *Chem. Phys. Lett.*, 1997, **274**, 242-250.

27. a. Andersen, N. G.; Keay, B. A.; *Chem. Rev.* **2001**, *101*, 997-1030; b. Dias, P.B.; Minas de Piedade, M. E.; Martino Simoes, J. A *Coord. Chem. Rev.* **1994**, *135/136*, 737-807.

28. a. Allman, T., Goel, R. G. *Can. J. Chem.* **1982**, *60*, 716-722; b. Bush, R. C.; Angelici, R. J. *Inorg. Chem.* **1988**, *27*, 681-686.

29. See supplementary material.

30. Atwood, J. D. *Inorganic and Organometallic Reaction Mechanisms, 2nd Ed.* Wiley-VCH, **1997**.

31. Mitchell, G. P.; Tilley, T. D. *J. Amer. Chem. Soc.* **1997**, *119*, 11236-11243.

32. Askham, F. R.; Saum, S. E.; Stanley, G. G. *Organometallics* **1987**, *6*, 1370-1372.

33. a. Treichel, P. M.; Vincenti, P.J. *Inorg. Chem.* **1985**, *24*, 228-230; b. Treichel, P. M.; Komar, D. A.; Vincenti, P. *Inorg. Chim. Acta* **1984**, *88*, 151-152; c. Haines, R. J.; DuPreez, A. L. *J. Organometal. Chem*. **1975**, *84*, 357-367.

ToC Graphic